PHYSICAL REVIEW B **70**, 121302(R) (2004)

Nonequilibrium electron transport using the density matrix renormalization group method

Peter Schmitteckert
Institut für Theorie der Kondensierten Materie, Universität Karlsruhe, 76128 Karlsruhe, Germany
(Received 22 March 2004; revised manuscript received 10 May 2004; published 8 September 2004)

We extended the density matrix renormalization group method to study the real time dynamics of interacting one-dimensional spinless Fermi systems by applying the full time evolution operator to an initial state. As an example we describe the propagation of a density excitation in an interacting clean system and the transport through an interacting nano structure.

DOI: 10.1103/PhysRevB.70.121302 PACS number(s): 73.63.Nm, 71.10.Fd, 71.10.Pm

I. INTRODUCTION

The density matrix renormalization group method (DMRG)[1,2] is a powerful technique to study the properties of one-dimensional interacting quantum systems. The advantage of the DMRG is that it can treat quantum lattice systems in the presence of site-dependent interaction, hopping parameters, and on-site potentials[3] with high accuracy, including subtle lattice effects like multiple umklapp processes.[4]

Originally, the method was set up to describe the equilibrium properties of the ground state and a few excited states. It was then extended to calculate frequency dependent spectral functions by the use of the $[H-E_0-\omega+\imath\eta]^{-1}$ operator.[5–7]

A second approach to study transport properties within the framework of DMRG is to relate equilibrium properties of the ground state to transport properties. Molina *et al.*[8] and Meden and Schollwöck[9] calculated the conductance through an interacting nano structure attached to leads by relating the conductance of the system to the ground state curvature, based on an idea by Sushkov.[10]

Cazalilla and Marston[11] used the basis states of the last DMRG step of the infinite lattice algorithm to integrate the Schrödinger equation in real time. However, since the initial state changes during the time evolution, this scheme works only for short time scales, since the inclusion of excited states, which are necessary for the long time evolution, into the set of basis states is not guaranteed and can be improved as shown by Luo, Xiang, and Wang.[12]

II. CALCULATION OF THE TIME EVOLUTION

Instead of integrating the time dependent Schrödinger equation numerically, we apply the time evolution operator

$$\mathcal{U}(t_2,t_1) = e^{-\imath\mathcal{H}(t_2-t_1)} \tag{1}$$

to calculate the time dependence of an initial state $|\xi(0)\rangle$,

$$|\xi(t)\rangle = \mathcal{U}(t,0)|\xi(0)\rangle, \tag{2}$$

where $\mathcal{H}$ is the Hamiltonian of the system of interest.

While the calculation of $e^{-\imath\mathcal{H}t}$ is not feasible for large matrix dimensions, one can calculate the action of a matrix exponential on a vector x very similar to Lanczos sparse matrix diagonalization.[13] For this purpose one calculates the full matrix exponential[14] $E^\ell = e^{\imath\mathcal{H}|_K^\ell}$, where $\mathcal{H}|_K^\ell$ is the projection of $\mathcal{H}$ onto the Krylov space $K_x^\ell(\mathcal{H}) = \mathrm{span}\{x, \mathcal{H}x, \mathcal{H}^2x \ldots \mathcal{H}^{\ell-1}x\}$. Starting with $\ell=5$ we iteratively increase ℓ until the residual $\Sigma_{j=\ell-2}^{\ell}|E_{j,1}^{\ell}|$ is below a desired threshold,[13,15,16] which we have set to 10^{-9}. The final result is then given by $e^{-\imath\mathcal{H}t}x = \|x\|\Sigma_{j=1}^{\ell}E_{j,1}^{\ell}b_j$, where b_j is a basis of $K_x^\ell(\mathcal{H})$ with $b_1 = x/\|x\|$.

In order to calculate $|\xi(t)\rangle$ up to a final time T, we discretize the time interval into N_T time steps $\{t_0, t_1, t_2 \ldots t_N\}$ with $t_0=0$, $t_j < t_{j+1}$ and $t_N = T$. It turns out that using a time slice $t_j - t_{j-1}$ of the order of one is sufficient to ensure a fast convergence, i.e., $\ell \sim 30$, of the iteration procedure which determines $|\xi(t_j)\rangle$,

$$|\xi(t_j)\rangle = e^{-\imath\mathcal{H}(t_j-t_{j-1})}|\xi(t_{j-1})\rangle. \tag{3}$$

Although one does not need to calculate the ground state of the unperturbed system, we calculate the m lowest lying eigenstates $|\Psi_m\rangle$ of $\mathcal{H}$, $E_m|\Psi_m\rangle = \mathcal{H}|\Psi_m\rangle$, and use the sparse matrix exponential only on the subspace orthogonal to these eigenstates,

$$\hat{P} = \sum_{m=0}^{m-1} |\Psi_m\rangle\langle\Psi_m|, \tag{4}$$

$$|\xi(t)\rangle = \sum_{m=0}^{m-1} e^{-\imath(E_m-E_0)t}|\Psi_m\rangle\langle\Psi_m|\xi(0)\rangle + e^{-\imath(\mathcal{H}-E_0)t}(1-\hat{P})|\xi(0)\rangle. \tag{5}$$

This projection improves the accuracy for very small perturbations. For strong perturbations we omit this projection. In addition we have introduced a phase choice of $e^{\imath E_0 t}$ to make the ground state time independent.

III. DMRG PROCEDURE

We use the well-established finite lattice DMRG algorithm,[2] where we target simultaneously $|\Psi_m\rangle$ and all $|\xi(t_j)\rangle$, i.e., we perform the full time evolution in each DMRG step. Specifically, we use the density matrix ρ to select the states

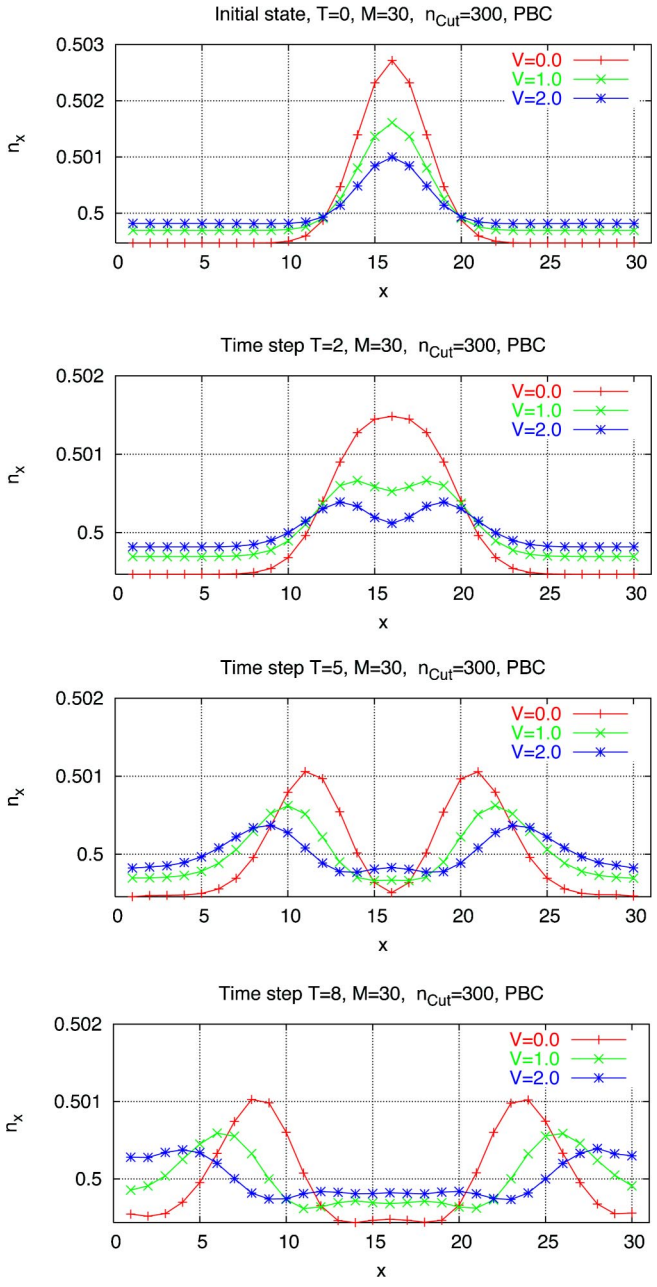

FIG. 1. (Color online) Time evolution of a wave packet for a system of $M=30$ sites, periodic boundary conditions, and $V=0.0$ (plus), $V=1.0$ (crosses) and $V=2.0$ (stars). The snapshots are taken at $t_j=0$, 2, 5, and 8. $n_{\mathrm{Cut}}=300$ states per block were kept within the DMRG procedure.

$$\rho = \mathrm{Tr}\left(\sum_m |\Psi_m\rangle\langle\Psi_m| + \sum_{j=0}^{N} |\xi(t_j)\rangle\langle\xi(t_j)| \right), \tag{6}$$

kept for the next iteration step, where the trace is taken over the states of the environment block,[2] and all operators, including the Hamiltonian used to calculate the time evolution, are updated in each DMRG step. In this work we always use $m=3$ low energy states and 11 finite lattice sweeps. Note that in the DMRG method, operators are evaluated in the subspace of the complete Hilbert space, which is targeted by the DMRG procedure.

TABLE I. Comparison of v_g extracted from DMRG simulations for a $M=30$ site system and a potential strength $\mu=0.02$, $\mu=0.002$ and Bethe ansatz results for v_F in the infinite system and an infinitesimal small excitation.

V	−1.5	0.0	0.5	1.0	1.5
v_g, $\mu=0.02$	1.0	1.9	2.2	2.47	2.71
v_g, $\mu=0.002$	0.92	2.00	2.30	2.59	2.87
v_F(BA)	0.88	2.00	2.31	2.60	2.88

IV. WAVE PACKET DYNAMICS

In order to prepare an initial state we apply a small perturbation $\delta\mathcal{H}$ to the Hamiltonian $\mathcal{H}$ of the system of interest and calculate $|\xi(0)\rangle$ as the ground state of $\mathcal{H}+\delta\mathcal{H}$.

As a first example we study the time evolution of a density pulse in a model of interacting spinless fermions:

$$\mathcal{H} = -\sum_{x=1}^{M} c_x^\dagger c_{x-1} + c_{x-1}^\dagger c_x + V\sum_{x=1}^{M}\left(n_x - \frac{1}{2}\right)\left(n_{x-1} - \frac{1}{2}\right), \tag{7}$$

where V denotes the nearest neighbor interaction parameter. In this work we measure all energies with respect to strength of the hopping parameter, which is set to one.

To create a wave packet we add a Gaussian potential

$$\delta\mathcal{H} = -\mu\sum_{x=1}^{M} \exp\left(-\frac{(x-x_1)^2}{2\sigma^2}\right) n_x, \tag{8}$$

where μ is the strength, σ the width, and x_1 the position of the perturbation. In Fig. 1 we have plotted the time evolution of an initial wave packet at $x_1=6$ in a 30 site system at half filling and periodic boundary condition using 300 states per DMRG block. Due to time reversal symmetry the initial state consists of a left and a right moving wave packet. During the time evolution the initial peak splits into two peaks which are moving with the group velocities $\pm v_g$. For $V=0$ the DMRG results coincide with the result from exact diagonalization. As a first result this method gives direct access to the group velocity v_g of a density excitation without relying on finite size analysis or arguments from conformal field theory.[17] In Table I we compare the extracted group velocities v_g for the $M=30$ site system with the Fermi velocity v_F known from Bethe ansatz results for an infinitesimal excitation in the infinite system size limit, $v_F=\pi\sin(2\eta)/(\pi-2\eta)$ with the usual parametrization $V=-2\cos(2\eta)$.[17] As expected from v_F the wave packets travel faster the stronger repulsive interaction are, while they are slowed down by attractive interaction. For $\mu=0.002$ there is a good agreement from v_g with v_F, while the results for $\mu=0.02$ already include dispersion effects. In addition, the broadening of the wave packets reveals information on the dispersion relation. A detailed study is beyond the scope of this work and subject for future studies.

It is not obvious that one can target for a few low lying states $|\Psi_m\rangle$ of $\mathcal{H}$, the ground state $\xi(0)$ of $\mathcal{H}+\delta\mathcal{H}$ and $N\sim 50$ time steps of $\xi(t_j)$ simultaneously in each DMRG step. However, since the DMRG truncation is the only approxima-

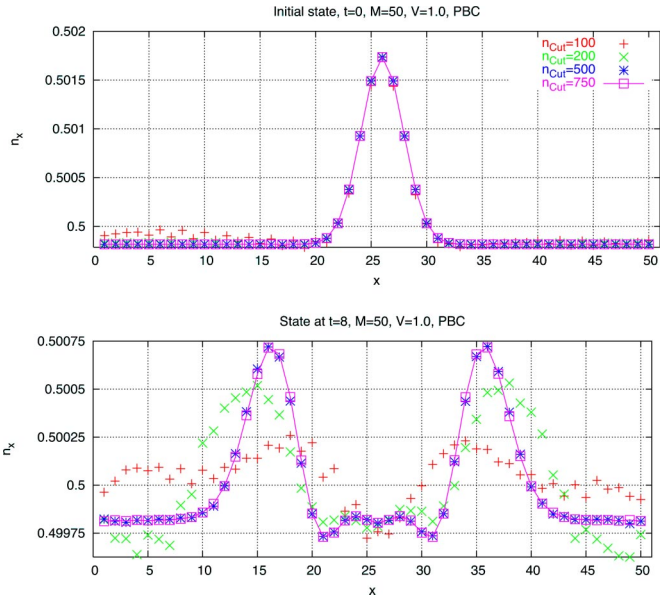

FIG. 2. (Color online) (a) Initial wave packet for a 50 site system with periodic boundary conditions and $V=1$, for different numbers of states kept per block: $n_{\mathrm{Cut}}=100$ (plus), 200 (crosses), 500 (stars) and 750 (open squares), extracted from a simulation with $T=20$ and time steps $t_j-t_{j-1}=1$. (b) Same system at time step $t_j=8$.

tion in our method, we can systematically increase the number of states n_{Cut} kept per block to control errors due to the Hilbert space truncation. In Fig. 2 we plot an initial wave packet $\xi(0)$ and a snapshot of $\xi(t)$ at $t_j=8$ for a 50 site system, a potential strength of $\mu=0.02$, an interaction of $V=1.0$, periodic boundary conditions and a simulation time of $T=20$. While for the initial state 200 states per block are sufficient to describe the wave packet, far more states are needed to obtain the dynamics of the wave packet correctly.

Remarkably, the overlap $\langle\Psi_0|\xi(0)\rangle$ between the ground state of $\mathcal{H}$ and the ground state of the system of $\mathcal{H}+\delta\mathcal{H}$ shown in Fig. 2 is 99.99%. Therefore, it is the 0.01% contribution which gives the initial excitation and governs the time evolution. This high overlap was the motivation to introduce the projection defined in Eq. (4).

V. TRANSPORT THROUGH A QUANTUM DOT

In order to study transport through an interacting nano structure, we prepare a system consisting of an interacting region coupled to noninteracting leads, see Fig. 3,

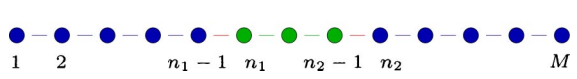

FIG. 3. (Color online) Nano structure attached to leads.

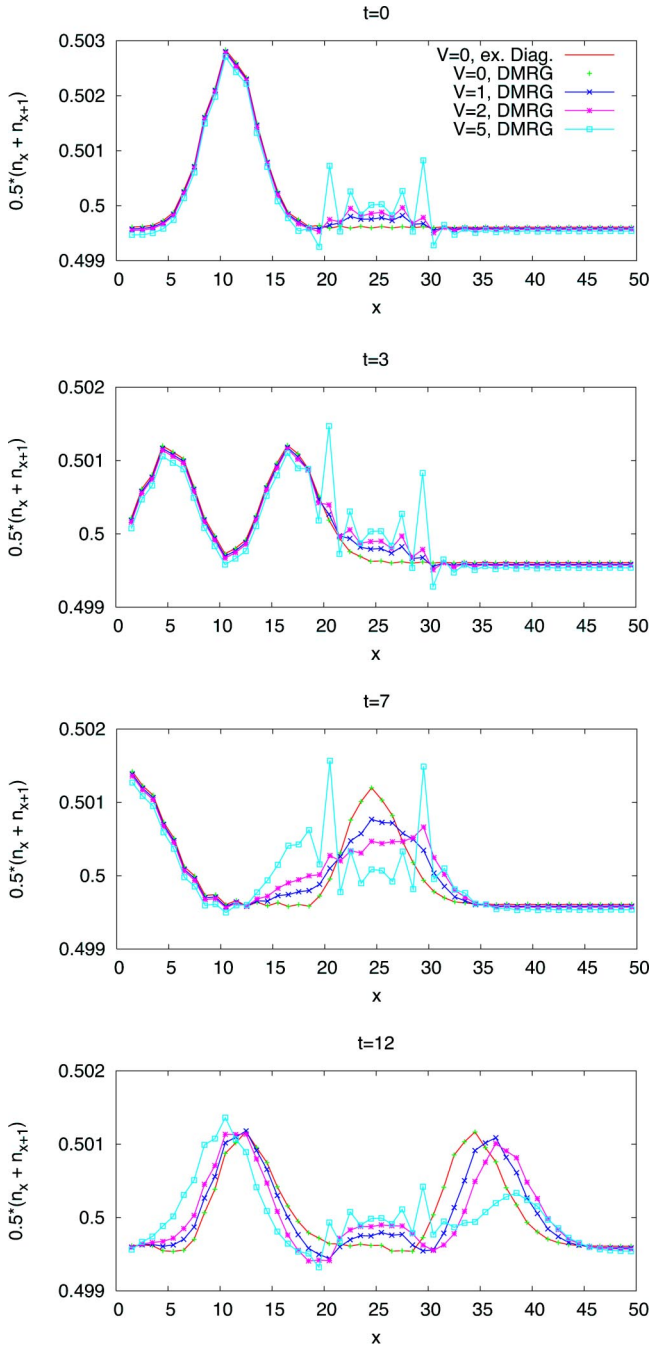

FIG. 4. (Color online) Transport through an interacting region of $M_S=7$ sites and $M_L=43$ lead sites, hard wall boundary conditions and $n_{\mathrm{Cut}}=1000$. The snapshots are taken at $T=0,3,7,12$. The density is averaged over two neighboring sites to smoothen $2k_F$ oscillations and is plotted vs the site location x for $V=0$ (plus), $V=1$ (crosses), $V=2$ stars, and $V=5$ (squares). For $V=0$ the line is calculated by an exact diagonalization.

$$\mathcal{H}=-\sum_{x=1}^{M}(c_x^\dagger c_{x-1}+c_{x-1}^\dagger c_x)+V\sum_{x=n_1+1}^{n_2-1}\left(n_x-\frac{1}{2}\right)\left(n_{x-1}-\frac{1}{2}\right)$$
$$+\gamma V\sum_{x=n_1,n_2}\left(n_x-\frac{1}{2}\right)\left(n_{x-1}-\frac{1}{2}\right), \qquad (9)$$

where the hopping parameter is set to one, U is the interac-

tion on the nano structure and γ defines a smoothening of the onset of interaction at the nano structure. In this work we have set $\gamma=0.5$, compare Molina *et al.*[8] In the following we denote $M_S=n_2-n_1$ the number of sites in the nano structure, M the number of site of the total system and $M_L=M-M_S$ the number of lead sites.

In Fig. 4 we show the time evolution of a wave packet initially placed in the left lead of a system with $M_S=7$, $M=50$, interaction $V=0.0$, 1.0, 2.0 and 5.0 and hard wall boundary conditions, which lead to perfect reflection at the chain ends. To rule out truncation errors we use $n_{\mathrm{Cut}}=1000$ states per block, compare the discussion of Fig. 2. We have averaged the density over neighboring sites to smoothen out the Friedel oscillations (for all V) and the charge density wave on the dot for $V=5.0$. At the beginning of the time evolution, the wave packet is not overlapping with the interacting nano structure, hence the packets travel synchronously for all interaction strength. Once they reach the nano structure, the wave packets move with the group velocity of the interacting system. After the wave packets have left the interacting region they continue to move at the velocity of the noninteracting system. The wave packets which traveled through the interacting region are now traveling in front of those with smaller interaction.

For $U\leqslant 2.0$ the nano structure is transparent, although there seems to be a reflection of a negative pulse as predicted by Safi and Schulz.[18] For very strong interaction, $U>2.0$, there is an instability to a charge density ordering,[4,17] and the nano structure has a finite reflection. We would like to remark that these simulations clearly demonstrate that the Luttinger description of the infinite system already makes sense for a system consisting of a few lattice sites only. One should keep in mind that for such small systems the effective parameters, like v_F, have not reached the infinite system limit. However, the scaling already leaves its fingerprint.

VI. SUMMARY

In summary we have shown an accurate method to calculate real time dynamics within the framework of DMRG. By applying the matrix exponential on an initial state we perform the complete time integration of the time dependent Schrödinger equation in each single DMRG step. In this setup the only approximation is given by the truncation procedure of the DMRG, which be can systematically checked by increasing the number of states kept. Therefore this method can be applied to strongly correlated systems even in the presence of strong perturbations. Using this method we have demonstrated that many particle correlations are already significant for transport properties for systems as small as seven sites.

Note added in proof. While preparing this work we became aware of related work[19,20] on using real time dynamics within the DMRG. Both apply a Suzuki-Trotter decomposition of the time evolution operator. In addition, their work relies on the state prediction[21] to calculate the time evolution of a state, which represents an additional approximation.

ACKNOWLEDGMENTS

I acknowledge the support of the Center for Functional Nano Structures within project B2.10. I would like to thank Karl Meerbergen for his hints on the matrix exponential and insightful discussions with Ralph Werner, Peter Wölfle, Gert L. Ingold, and Rudolf Lohner.

[1] S. R. White and R. M. Noack, Phys. Rev. Lett. **68**, 3487 (1992); S. R. White, *ibid.* **69**, 2863 (1992); Phys. Rev. B **48**, 10 345 (1993).

[2] *Density Matrix Renormalization—A New Numerical Method in Physics*, edited by I. Peschel, X. Wang, M. Kaulke, and K. Hallberg (Springer, Berlin, 1999).

[3] P. Schmitteckert, T. Schulze, C. Schuster, P. Schwab, and U. Eckern, Phys. Rev. Lett. **80**, 560 (1998); P. Schmitteckert, R. A. Jalabert, D. Weinmann, and J. L. Pichard, *ibid.* **81**, 2308 (1998).

[4] P. Schmitteckert and R. Werner, Phys. Rev. B **69**, 195115 (2004).

[5] K. A. Hallberg, Phys. Rev. B **52**, R9827 (1995).

[6] T. D. Kühner and S. R. White, Phys. Rev. B **60**, 335 (1999).

[7] E. Jeckelmann, Phys. Rev. B **66**, 045114 (2002).

[8] R. A. Molina, D. Weinmann, R. A. Jalabert, G.-L. Ingold, and J.-L. Pichard, Phys. Rev. B **67**, 235306 (2003).

[9] V. Meden and U. Schollwöck, Phys. Rev. B **67**, 193303 (2003).

[10] O. P. Sushkov, Phys. Rev. B **64**, 155319 (2001).

[11] M. A. Cazalilla and J. B. Marston, Phys. Rev. Lett. **88**, 256403 (2002).

[12] H. G. Luo, T. Xiang, and X. Q. Wang, Phys. Rev. Lett. **91**, 049701 (2003).

[13] Y. Saad, SIAM (Soc. Ind. Appl. Math.) J. Numer. Anal. **29**, 130 (1998).

[14] We would like to encourage the reader to study the excellent review by Moler and Van Loan (Ref. 15). In our implementation we utilize a Padé approximation from EXPOKIT (Ref. 16) to calculate the matrix exponential in the Krylov space.

[15] C. Moler and C. Van Loan, SIAM Rev. **45**, 3 (2003).

[16] R. B. Sidje, EXPOKIT–*A software package for computing matrix exponentials*, ACM Trans. Math. Softw. **24**, 130 (1998).

[17] V. E. Korepin, N. M. Bogoliubov, and A. G. Izergin, *Quantum Inverse Scattering Method and Correlation Functions* (Cambridge University Press, Cambridge, 1993).

[18] I. Safi and H. H. Schultz, in *Quantum Transport in Semiconductor Submicron Structures*, edited by B. Kramer (Kluwer Academic, Dordrecht, 1995).

[19] S. R. White and A. E. Feiguin, Phys. Rev. Lett. **93**, 076401 (2004).

[20] A. J. Daley, C. Kollath, U. Schollwoeck, and G. Vidal, cond-mat/0403313.

[21] S. R. White, Phys. Rev. Lett. **77**, 3633 (1996).